TECTONICS, VOL. 17, NO. 6, PAGE 859-871, DECEMBER, 1998

Plate-boundary strain partitioning along the sinistral collision suture of the Philippine and Eurasian plates: Analysis of geodetic data and geological observation in southeastern Taiwan

Jian-Cheng Lee,[1] Jacques Angelier,[2] Hao-Tsu Chu,[3] Shui-Beih Yu,[1] and Jyr-Ching Hu[1]

Abstract. Crustal deformation and strain partitioning of oblique convergence between the Philippine Sea plate and the Eurasian plate in the southern Longitudinal Valley of eastern Taiwan were characterized, based on geodetic analysis of trilateration network and geological field investigation. The Longitudinal Valley fault, one of the most active faults on Taiwan, branches into two individual faults in the southern Longitudinal Valley. These two active faults bound the Plio-Pleistocene Pinanshan conglomerate massif between the Coastal Range (the Luzon island arc belonging to the Philippine Sea plate) and the Central Range (the metamorphic basement of the Eurasian plate). A geodetic trilateration network near the southern end of the valley shows a stable rate of the annual length changes during 1983-1990. The strain tensors for polygonal regions (including triangular regions) of the Taitung trilateration network reveal that there are two distinct zones of deformation: a zone of shortening (thrusting) between the Pinanshan massif and the Central Range on the west, and a strike-slip movement between the Pinanshan massif and the Coastal Range on the east. The analysis of a discontinuity model consisting of three-rigid-blocks separated by two discontinuities has been carried out. The results show that the deformation in this region can be characterized by two major faults. A reverse fault is located between the Plio-Pleistocene Pinanshan massif and the metamorphic basement of the Central Range, with a shortening rate of about 12 mm/yr in the direction N280°E. A strike-slip fault is located principally along the river between the Pinanshan massif and island arc system of the Coastal Range with an purely strike-slip component of about 22 mm/yr in the direction N353°E. The analysis of the geodetic data analysis further suggests that substantial deformation (probably strike-slip in type) occurs within the Pinanshan massif. Geological evidence of deformation in the Plio-Pliestocene Pinanshan conglomerate includes regional folding, conjugate set of strike-slip fractures at the outcrop scale, and morphological lineaments related to fracturing, all indicating that the Pinanshan massif is being deformed within a transpressive stress regime. Regional kinematic data indicate that a significant portion of the 82 mm/yr of motion between the Eurasian plate and the Philippine Sea plate is absorbed in the southern Longitudinal Valley by the decoupling of two distinct major faults. The geometry of the oblique convergence and the rheology of the rock units (the well-consolidated Plio-Pleistocene conglomerate and the sheared mélange formation) play the two important factors in the partitioning of crust deformation.

[1]Institute of Earth Sciences, Academia Sinica, P.O. Box 1-55, Nankang, Taipei, Taiwan, R.O.C.

[2]Géotectonique (URA 1759), Univ. P. & M. Curie, 4 pl. Jussieu, T26-25-E1, 75252 Paris, France.

[3]Central Geological Survey, P.O. Box 968, Taipei, Taiwan, R.O.C.

Paper number 98TC02205.
0278-7407/98/98TC-02205$12.00

1. Introduction

Deformation adjacent to large crustal-scale strike-slip faults within a region of transpressive stress has been interpreted in two different manners [Mount and Suppe, 1992]. The first interpretation involves wrench tectonics with relatively strong coupling along fault systems [Wilcox *et al*., 1973] leading to oblique slip. In contrast, the second model involves decoupling of oblique convergence into components of thrust and strike-slip faulting [Fitch, 1972], which results in partitioning of stress and strain. Regions of decoupling of active transpressive faulting are often characterized by the major strike-slip fault and associated compressional structures which generally show a high angle between the principal stress direction and the major fault orientation. Analyses of stress fields [Mount and Suppe, 1987, 1992; Zoback *et al*., 1987] effectively revealed the common presence of decoupling across active transpressive plate boundaries, such as observed along the San Andreas fault, Great Sumatran fault, Alpine fault, and Philippine fault. In this paper, we aim at presenting the characteristics of strain partitioning and decoupling of strike-slip faulting and thrusting in an active suture zone in eastern Taiwan. This partitioning is caused by the convergence between the Luzon island-arc system of the Philippine Sea plate and the Chinese continental margin of the Eurasian plate (Figure 1), which is oblique to the plate boundary. This study presents geophysical and geological evidence, which includes analysis of geodetic trilateration measurement, field structural analysis, and morphological study based on remote sensing data.

The Taiwan orogenic belt is the product of the convergence between the Philippine Sea plate and the Eurasian plate. The relative plate motion is 70 km/My in the direction N310°E according to Seno and others [1987]. Recent estimates of the displacement between the islands of the Philippine Sea plate (Lutao and Lanhsu) and those of the Taiwan Strait (Penghu) has revealed a velocity of 8.2 cm/yr in the N309°E direction [Yu *et al*., 1997] (Figure 1a).

The recent mountain building process resulted from this plate convergence in the Taiwan area began about 5 Ma and is still active. The Longitudinal Valley (Figure 1b), trends NNE-SSW in eastern Taiwan; it has commonly been interpreted as the active suture zone [Ho, 1986], which links the Ryukyu trench-arc system to the north with the Luzon arc-Manila trench system to the south. To the west of the Longitudinal Valley, Pre-Neogene (mostly late Paleozoic/Mesozoic basement) metamorphic rocks belong to the Central Range. To the east, the Miocene volcanic arc and overlying Plio-Pleistocene sediments form the Coastal Range. The Longitudinal Valley forms a narrow zone from one to several

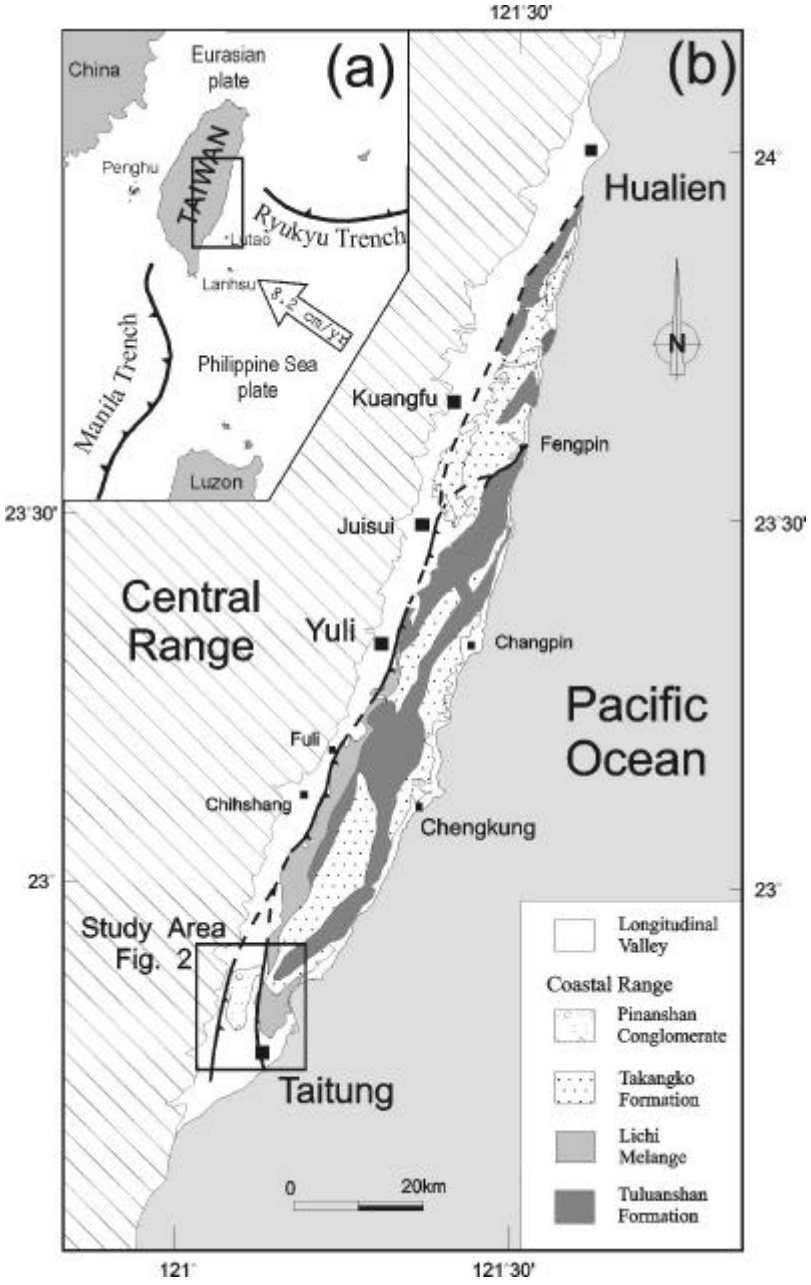

Figure 1. (a) Convergence between the Philippine Sea plate and the Eurasian plate in the Taiwan area. Arrow indicates the relative vector across Taiwan island with 8.2 cm/yr in the direction N309°E [Yu et al., 1997]. (b) General geological map of the Coastal Range in eastern Taiwan [Ho, 1988]. Thick solid and dashed lines represent the traces of the active Longitudinal Valley Fault.

kilometers wide that is the site horizontal crustal shortening of about 20 mm/yr [Yu *et al.*, 1990; Lee and Angelier, 1993]. The deformation zone along the Longitudinal Valley corresponds to the area of greatest crustal shortening throughout the Taiwan mountain belt and represents approximate 25-30% of the total plate convergence between the Luzon island arc of the Philippine Sea plate and the Chinese continental margin of Eurasia.

The large amount of crustal shortening in the active suture zone of the Longitudinal Valley is principally accommodated by active faulting of the Longitudinal Valley Fault, which reveals substantially different slip vectors along the length of the Longitudinal Valley based on the analysis of repeated trilateration data [Yu *et al*., 1990]. At the northern tip of the Longitudinal Valley near Hualien (Figure 1b), the Longitudinal Valley Fault consists of a strike-slip fault with left-lateral slip of about 23 mm/yr [Yu *et al*., 1990]. In the middle part of the valley from Juisui to Chihshang (Figure 1b), the Longitudinal Valley Fault acts as a left-lateral reverse fault (2/3 of transverse component and 1/3 of strike-slip component) with about 21 mm/yr of oblique horizontal shortening [Yu and Liu, 1989; Lee and Angelier, 1993]. In the southern part of

the valley, the Longitudinal Valley Fault shows a total horizontal shortening of 34 mm/yr (Yu *et al*., 1990). Oblique shortening in this region is apparently accommodated along two branches of the fault (a reverse fault and a strike-slip one, Figure 1b), located on both sides of the Plio-Pleistocene molasse deposits (Pinanshan Conglomerate) between the Central Range and the Coastal Range.

Our study examined the southern part of the Longitudinal Valley near Taitung (Figure 2) where crustal deformation is decoupled into thrust and strike-slip component. This region provides a good opportunity for understanding decoupling and strain-stress partitioning within an active oblique collision. The purpose of this paper is to present new observations, based on field geological investigations and photo-image interpretation. Modeling geodetic data also supports these observations. A decoupling model is proposed, in order to elucidate the partitioning of strain within the crustal shear zone between the converging Philippine Sea plate and Eurasian plate.

2. General geology

The Longitudinal Valley separates the Neogene island arc of Luzon exposed in the Coastal Range and the Pre-Tertiary metamorphic basement and overlying Paleogene slate of the Eurasian plate in the Central Range. In the southern Longitudinal Valley, near Taitung (Figure 2a), the Pinanshan Conglomerate

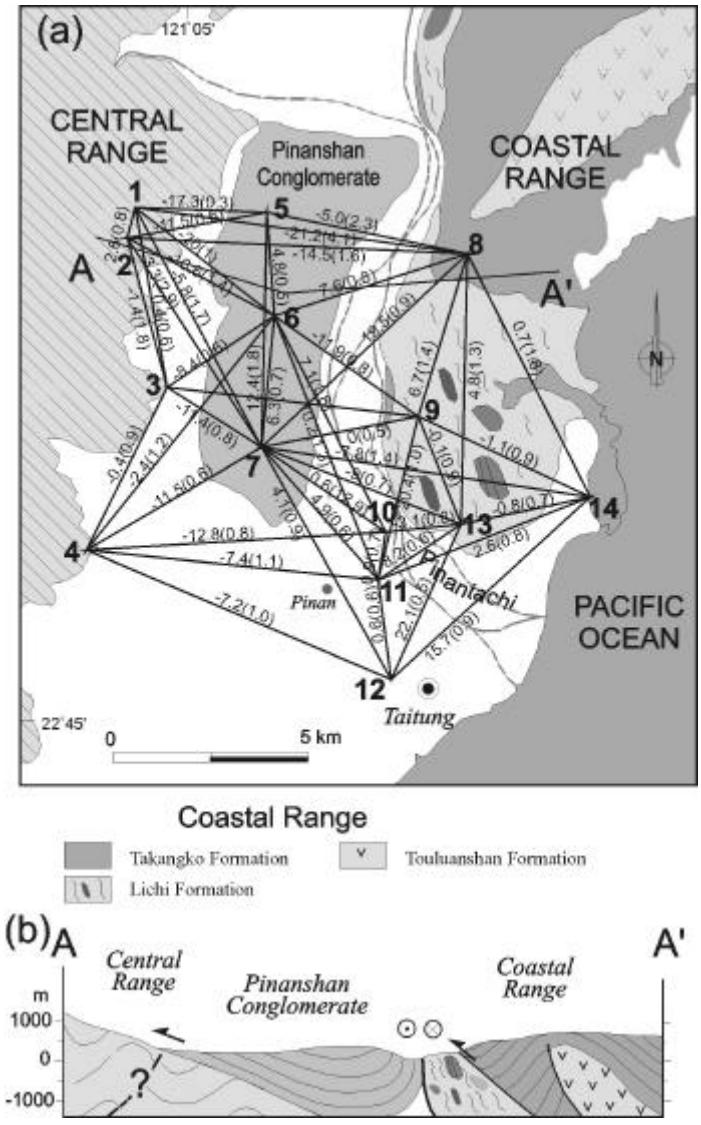

Figure 2. (a) Geological map and trilateration network in the southern Longitudinal Valley. Annual average length changes in the network are shown for each segment, with standard errors in the parentheses (value in mm). Values are negative for shortening, positive for lengthening. (b) Geological cross-section in the southern Longitudinal Valley. The vergence of the thrust on the western side of the Pinanshan Conglomerate is still unknown (question mark in section), although westward thrusting seems more likely (half-arrow).

forms a molasse deposit between the Coastal Range and the Central Range.

2.1. Coastal Range

The Coastal Range can generally be divided into three rock units: (1) the Tuluanshan Formation, with Miocene andesitic volcanic rocks [Hsu, 1956; Yang *et al*., 1995], constituting the basement of the Coastal Range; (2) the Takangkou Formation, with Plio-Pleistocene flysch-type deposits, overlying the Tuluanshan volcanic basement [Teng and Wang, 1981; Huang *et al*., 1995]; (3) the Lichi Formation, a Pliocene mélange formation composed of numerous exotic blocks of continental and ophiolitic origins within a sheared muddy matrix, situated principally on the western edge of the Coastal Range near to the Longitudinal Valley [Hsu, 1976; Page and Suppe, 1981].

The Coastal Range exhibits numerous west-vergent thrusts, generally striking NNE-SSW, parallel or sub-parallel to the trend of the Longitudinal Valley. Within these thrust blocks, the overlying Takangkou sedimentary units are deformed and folded.

In the study area, the Lichi mélange crops out to the east of the Pinantachi River whereas the Pinanshan Conglomerate is exposed to the west (Figure 2). Numerous striated micro-faults within the Lichi mélange suggest strong shearing during the convergence between the Luzon island arc (the Coastal Range) and the Central Range [Barrier and Muller, 1984]. However, another interpretation considers the Lichi mélange to be a large olistostrome [Page and Suppe, 1981], suggesting that shearing is related to gravity sliding rather than to plate convergence. These interpretations are not mutually exclusive.

2.2. Central Range

The pre-Neogene metamorphic rocks of the Central Range are situated to the west of the Longitudinal Valley. In the Taitung area, the east edge of the Central Range principally is composed of highly deformed low grade Paleogene slate (or phyllite) and quartz-feldspars metasandstone, Hsinkao Formation [Stanley *et al*., 1981]. The Paleogene slate is underlain by the Pre-Tertiary high grade Tananao complex is composed of marble, green schist, quartz-mica schist, and granitoid rocks, which are believed to be Permian to Cretaceous in age [Yen, 1951; Chen, 1989] as the basement of the Eurasian plate in Taiwan. The metamorphism of the Central Range is generally in two major events of late Mesozoic and Plio-Pleistocene [Jahn *et al*., 1986]. The general orientation of the metamorphic foliation along the eastern part of the Central Range is NNE-SSW and dipping moderately to the west [Stanley *et al*., 1981] in the study area.

2.3. Pinanshan Conglomerate

The Pinanshan Conglomerate lies in the southern end of the Longitudinal Valley (Figure 2a) along the western side of the Pinantachi River, which separates the Coastal Range (to the east) and the Pinanshan Conglomerate (to the west). Much smaller, discontinuous valleys, on the other hand, exists to the west, between the Pinanshan Conglomerate and the Central Range. As a consequence, the Pinanshan Conglomerate constitutes a topographic massif within the Longitudinal Valley.

The Pinanshan Conglomerate is composed of an accumulation of coarse fluvial sediments [Hsu, 1956; Teng and Wang, 1981; Page and Suppe, 1981; Barrier *et al*., 1982], which were deposited at the foot of the Central Range. The total thickness of the Pinanshan Conglomerate is more than 2000 meters, though the complete sedimentary sequence is not entirely exposed. The majority of clasts within the Pinanshan Conglomerate derived from the metamorphic units of the Central Range, whereas clasts from the Coastal Range are present but few, implying that the depocenter of the Pinanshan Conglomerate was closer to the Central Range (to the west) than to the Luzon arc. The proto-Coastal Range, which was at the beginning stage of uplift during collision process, was for most part under the sea level during the deposition of the Pinanshan Conglomerate.

Lack of paleontological data, the accurate age of the Pinanshan Conglomerate remains uncertain, though reworked late Miocene nannofossils have been found in shale layers of the unit [Chi *et al*., 1983]. In the adjacent area, the Takangkou flysch Formation of the Coastal Range reveals several periods of rapid deposition with coarse sediments [Horng and Shea, 1996; Horng *et al*., 1997], indicating probable major tectonic events. The Pinanshan Conglomerate, with coarse terrestrial deposits, could thus be compared to and be related to one of these stratigraphic/tectonic events.

The Pinanshan Conglomerate has deformed into an asymmetrical syncline (Figure 2b), with a slightly dipping western limb and steeply to vertically dipping layers in the eastern limb. The western side of the Pinanshan Conglomerate is in contact with schistose rocks of the Central Range (Figure 2a). The eastern limb of the fold is exposed in a cliff along bank of Pinantachi River and shows vertical and sometimes overturned conglomerate beds.

3. Geodetic data analysis

Our work of geodetic data analysis including strain tensor determination and discontinuous model analyses is based on data collected by Yu *et al*. [1992], using the Taitung trilateration network (Figure 2) situated on the southern extremity of the Longitudinal Valley. The network extends across three major tectonic units: from east to west, the Coastal Range, the Longitudinal Valley (including the Pinanshan Conglomerate), and the Central Range.

Each line of the trilateration network has been measured annually between 1983 and 1990 with a medium-range electronic distance meter [Yu *et al*., 1992]. The precision of the measurements over distances of 1-12 kilometers is represented by a standard deviation $\sigma=(a^2+b^2L^2)^{1/2}$, where a=3mm, b=0.7ppm, and L is the line length. Details of the survey procedures and precision of the trilateration network have been described before [Lee and Yu, 1985; Yu *et al*., 1992]. The results of the Taitung trilateration network have been summarized in terms of average annual length changes for 48 measured lines in the network [Yu et al., 1992]. Annual data showed relatively stable rates of length changes within the Taitung network between 1983 and 1990 [Yu et al., 1992].

3.1. Strain tensor analysis

We first undertook a 'classical' analysis in terms of strain tensor, using the data of the annual average rate of length changes in the Taitung trilateration network. Here we do not enter into the detail for

the algorithms of the calculation of strain tensor, which has been documented before [Lee and Angelier, 1993] and is described here in the appendix. Instead of reconstructing the average strain tensor for the whole network [e.g., Yu *et al*., 1992], we first calculated the local strain tensors by dividing the network into several triangles (Figure 3). Each triangle is assigned a strain tensor which represents average local deformation within the triangle area. Note that we did not consider the network deformation to be plane-strain; we considered it as the expression in the horizontal plane of a 3-dimensional strain (in which one principal axis is vertical). This is the reason why the maximum and minimum principal strains may have the same sign in the calculation.

Table 1 shows that some strain tensors estimated in triangles have large uncertainties whereas other ones are tightly constrained. For instance, the triangle 7-10-13 reveals large uncertainty in terms of e, the triangle 7-10-11 reveals large uncertainty in terms of e and q. The reason for obtaining large uncertainties lies in the original geodetic data, especially along line 7-10 (Figure 2a) where a poorly constrained datum was obtained.

On the other hand, the determinations in triangles use only three length changes for solving the three unknowns of the strain tensor. For this reason, we also determined the strain tensors in polygon areas (Figure 3b), which provide a smaller number of determination in a larger areas, hence generally smaller uncertainties of the results (Tables 1 and 2; see Figure 3 for comparison).

The results of the strain tensor analysis (Figure 3 and Table 1) show that the crustal deformation in the area of the Taitung trilateration network generally illustrates two major different styles prevailing along the eastern and western sides of the Pinanshan massif. The western part of the survey area exhibits a distinctive zone of E-W to ESE-WNW horizontal shortening between stations in the Pinanshan Conglomerate and stations in the Central Range (Figure 3). In contrast, the triangles on the eastern part of the network show a variety of strain tensors, with horizontal deformation being generally represented by a combination of NW-SE shortening and NE-SW elongation, except on the southeastern part where extension prevails (Figure 3, Tables 1 and 2). The stations in the southeast are located within mélange of Lichi Formation, which is composed of large exotic blocks within the sheared muddy matrix, probably leading to locally heterogeneous deformation.

The E-W to ESE-WNW shortening between the Pinanshan Conglomerate and the Central Range is generally perpendicular to the boundary between these two units (trending NNE-SSW; Figure 3). This indicates possible thrusting along an E-W to ESE-WNW direction between the Pinanshan Conglomerate and the Central Range. On the other hand, strain with NW-SE shortening and NE-SW elongation in the eastern part corresponds to a stress regime of strike-slip fault zone which trends N-S along the boundary between the Coastal Range and the Pinanshan Conglomerate. Taking into account geological observations (see a later section), which show that a major discontinuity existed between the Coastal Range and the Pinanshan Conglomerate, one observes that the deformation in the eastern part of the study area concentrates in this N-S to NNE-SSW trending zone. The N-S to NNE-SSW fault zone under a transpressive strain with NW-SE shortening and NE-SW elongation hence results in a left-lateral strike-slip. As a consequence, the strain tensors in the southern Longitudinal Valley are mechanically consistent with the presence of two major fault systems, (1) thrusting between the Pinanshan Conglomerate and the Central Range, and (2) left-lateral strike-slip faulting between the Pinanshan Conglomerate and the Coastal Range.

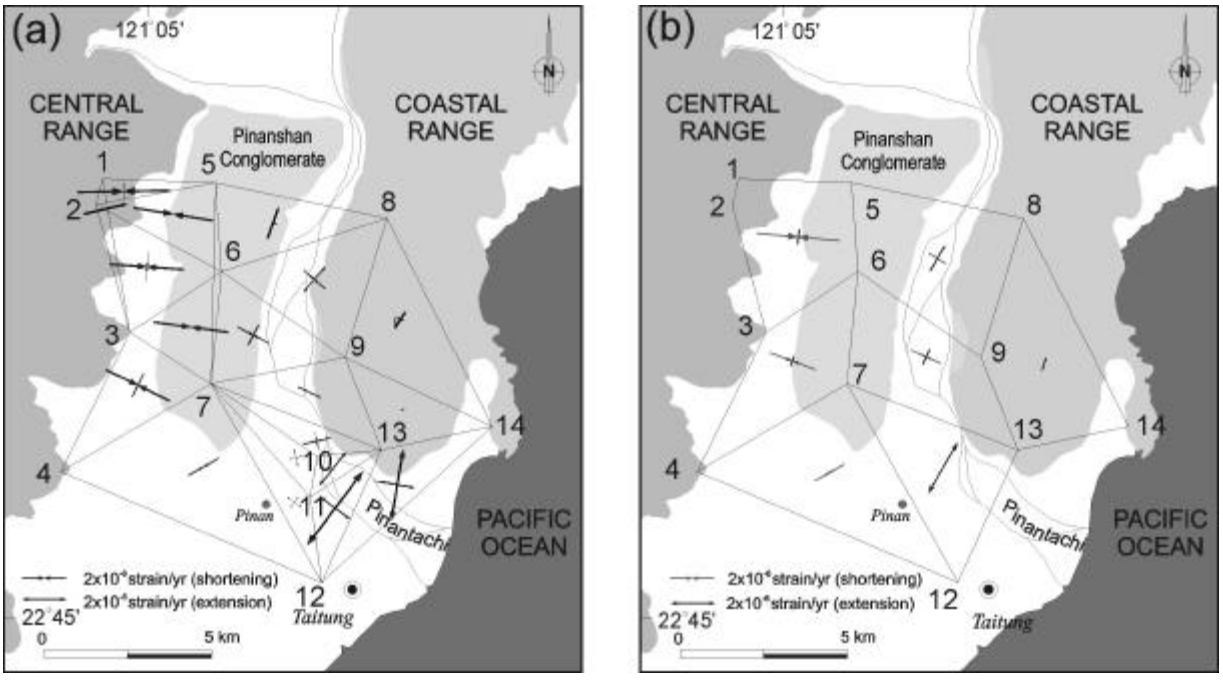

Figure 3. Strain tensor analysis of the Taitung trilateration network. (a) Strain tensors for triangular regions. (b) Strain tensors for polygonal regions. Explanation in text. The deformation for each triangle or polygon is represented by a 2-D strain tensor. Arrows indicate the principal components of the strain tensor (divergent for extension, convergent for shortening). Scales of strain rate in lower left corner. See also Tables 1 and 2.

Table 1. Results of Analysis of Strain Tensors for Triangular Areas in the Taitung Trilateration Network.

Triangle	ε_1 ($\times 10^{-6}$)	standard error of ε_1 ($\times 10^{-6}$)	ε_2 ($\times 10^{-6}$)	standard error of ε_2 ($\times 10^{-6}$)	θ(°)	standard error of θ(°)
1-2-3	2.061	0.788	-0.055	0.279	166.6	0.4
1-2-5	0.713	0.71	-4.118	0.133	88.8	0.2
2-5-6	0.014	0.202	-3.561	0.258	99.5	0.7
2-3-6	-1.292	0.372	-3.298	0.28	94.4	1.8
3-6-7	0.196	0.227	-3.337	0.318	98.4	0.9
3-4-7	-1.099	0.179	-3.132	0.311	116.5	0.9
5-6-8	1.534	0.193	0.029	0.335	109.5	0.8
6-8-9	1.490	0.241	-1.249	0.2	131.1	1.0
6-7-9	1.059	0.178	-1.588	0.165	117.4	0.5
7-9-13	-0.035	0.223	-1.098	0.15	114.8	2.0
7-10-13	-0.826	1.71	-1.259	0.92	77.5	2.6
7-10-11	0.748	0.91	0.547	1.827	78.2	24.2
7-11-12	0.550	0.19	0.749	0.147	125.5	5.4
4-7-12	-0.112	0.128	-1.548	0.119	61.0	0.1
10-11-13	1.905	0.343	-0.329	0.476	129.3	1.8
11-12-13	4.134	0.161	1.614	0.133	127.4	0.4
12-13-14	3.247	0.136	1.555	0.169	99.7	0.3
9-13-14	-0.11	0.268	-0.225	0.201	89.7	2.3
8-9-14	0.944	0.287	0.012	0.23	123.3	0.9

ε_1: the maximum principal strain axis, ε_2: the minimum principal strain axis. θ the azimuth of the minimum principal strain axis.

3.2 Discontinuous model analysis

A discontinuous model analysis was used to interpret the results of the trilateration network and to illustrate quantitatively the characteristics of the surface crustal deformation along highly localized active faulting. In the case of this discontinuous model, the deformation is simply represented by the relative movement of rigid blocks separated by rectilinear fault [Lee and Angelier, 1993]. The horizontal movement is defined by two series of variables: amount and direction of the relative movement. These variables, together with the location of the discontinuity (fault), are considered through an inversion technique, in order to reconstruct a regional deformation model. The vectors of displacement, $\vec{L}_k^*$, for each line in the trilateration network, are compared with the calculated vectors, $\vec{L}_k$, produced by the discontinuous model. The sum of the difference, *S*, between these two vectors, for all the line segments in the network, can be minimized through a least square-root method. The details of the method are shown in Appendix.

Two major active faults have been identified in the study area based on field investigation. These faults compose branches of the Longitudinal Valley Fault in the southernmost extent of the Longitudinal Valley. The two faults divide the area into three blocks: from west to east, the Central Range, the Pinanshan Conglomerate, and the Coastal Range. In addition to these two major discontinuities, an analysis of SPOT imagery reveals that two distinct linear structures cut across the Pinanshan Conglomerate (Figure 4). Yü [1996] identified two active conjugate strike-slip faults (a right-lateral fault trending approximately N95°E in the north and a left-lateral fault trending about N140°E in the south), which may correspond to the two major lineaments observed in SPOT image (Figure 4).

Three problems of discontinuous behavior deserve consideration in our model: (1) the location of the main western discontinuity, (2) the location of the main eastern discontinuity, and (3) the possible presence of additional discontinuities within the Pinanshan massif. As a first approximation, we started our analysis with a model of three rigid blocks with two major discontinuities, ignoring the additional effects related to deformation within the Pinanshan

Table 2. Results of Analysis of Strain Tensors of Polygons in the Taitung Trilateration Network

Polygon	ε_1 ($\times 10^{-6}$)	standard error of ε_1 ($\times 10^{-6}$)	ε_2 ($\times 10^{-6}$)	standard error of ε_2 ($\times 10^{-6}$)	θ(°)	standard error of θ(°)
1-2-3-5-6	-0.734	0.246	-3.796	0.207	94.6	0.5
3-4-6-7	-0.496	0.185	-2.232	0.271	109.8	1.7
5-6-8-9	1.373	0.255	-0.904	0.287	120.6	0.0
6-7-9-13	0.822	0.203	-1.511	0.156	114.2	0.6
7-13-10-11-12	2.657	0.199	-0.037	0.621	119.9	0.1
8-9-13-14	0.644	0.239	-0.040	0.220	107.4	0.6

ε_1: the maximum principal strain axis, ε_2: the minimum principal strain axis. θ: the azimuth of the minimum principal strain axis.

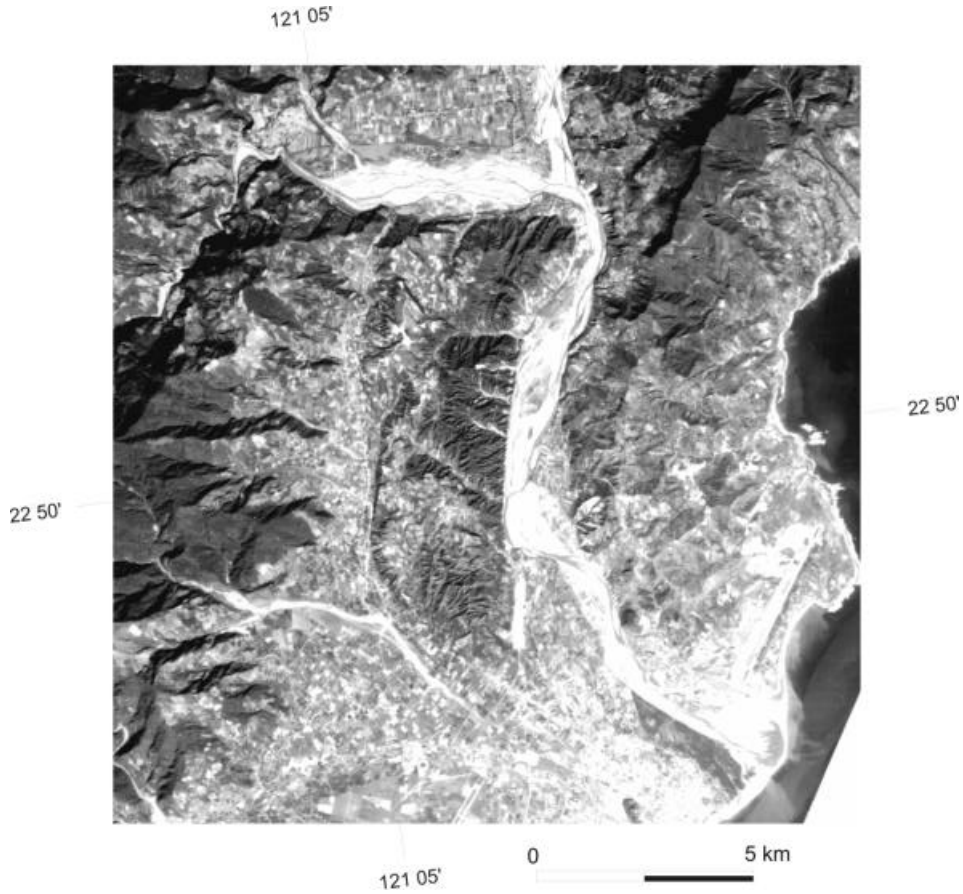

Figure 4. SPOT image of the area of the southern Longitudinal Valley. Note the linear structures along the eastern edge of the Pinanshan Conglomerate and the western edge in the southern part. Two main drainage alignments in the Pinanshan Conglomerate (trending N95°E in the north and N140°E in the south) possibly reveal major strike-slip faults.

Conglomerate.

For the location of the main western discontinuity, we adopted the boundary between the Central Range and the Pinanshan Conglomerate, as indicated by the geological evidence and by the above strain tensor analysis. On the other hand, on the eastern part of the area, although there exists substantial deformation generally between the Pinanshan Conglomerate and the Coastal Range (Figure 3), the location of the discontinuity remained unclear in the southeastern part of the network. As a result, we introduced a particular computer process in order to search automatically for active discontinuities within the network by minimizing the sum of the differences between the measured data and the length changes deduced from the model. The uncertainty of the solutions has been estimated by introducing the standard errors of the measured data (Figure 2).

The results of the analysis of this discontinuous model indicate that the Pinanshan Conglomerate moved westward toward the Central Range with a rate of 10±3 mm/yr in the direction of N280±20°E and the Coastal Range moved northward compared to the Pinanshan Conglomerate (Figure 5) with a rate of 22±5 mm/yr in the direction of N353±7°E. The discontinuity, which trends N-S and is found to be a left-lateral strike-slip fault, generally lies along the Pinantachi River, between the Pinanshan Conglomerate and the Coastal Range, and passes between station 10 and station 13 (Figures 2 and 5). The two major displacements produce a total vector of 28 mm/yr in the direction N329°E (Figure 6), which represents the total displacement across the Longitudinal Valley between the Central Range and the Coastal Range.

The displacements calculated with the discontinuous model have then been applied to the trilateration network system to determine theoretical length changes for each line of the geodetic network (Figure 5). Comparing these calculated changes with the real data (Figure 5a) revealed by the histograms (Figure 5b), one observes that the induced length changes are generally in a good agreement with the measured ones (the differences between the measured data and the calculated ones are basically restricted within ±5 mm/yr, see Figure 5c).

The misfits lie essentially on lines related to the stations within the Pinanshan Conglomerate (Figure 5). This indicates that substantial deformation exists within the Pinanshan Conglomerate. We take into account the major alignments in the Pinanshan massif, as revealed by the morpho-geological data mentioned before (Figure 4, with N95°E trends in the north and N140°E trends in the south). Therefore, the N140°E trending alignment in the southern Pinanshan Conglomerate probably acts as a locally significant left-lateral strike-slip fault. Displacements and strain tensors consistently show a N-S to NNW-SSE elongation and E-W to ESE-WNW shortening around the Pinanshan Conglomerate, implying left-lateral strike-slip fault(s) between the northernmost station and the middle one. Another

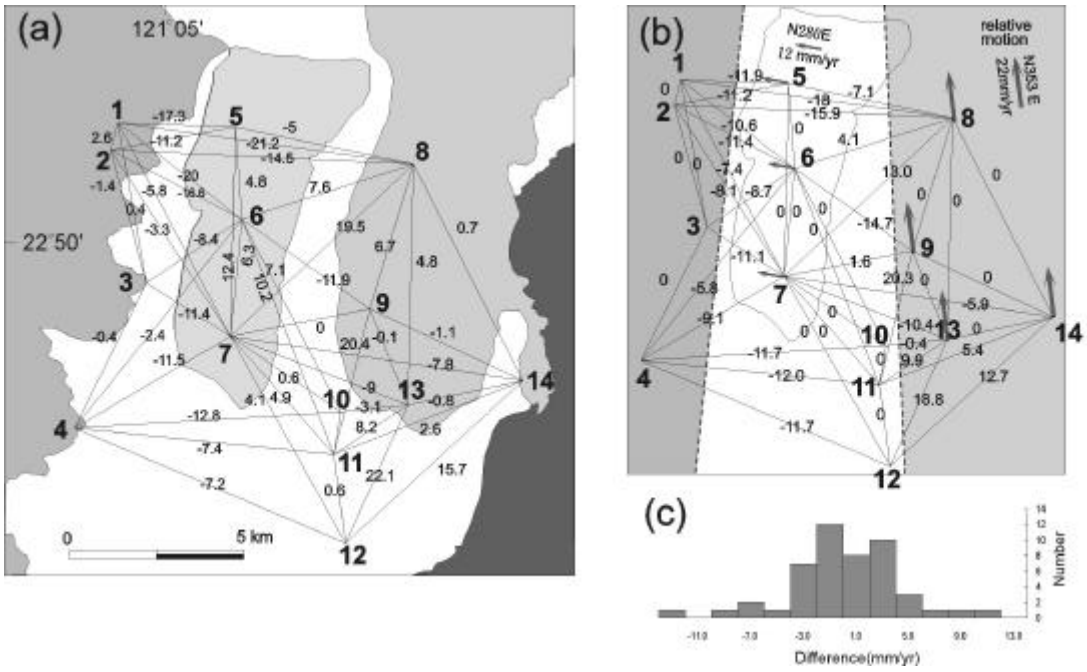

Figure 5. Geodetic analysis of the discontinuous model in the Taitung trilateration network. (a) Data of length changes obtained from trilateration measurements [Yu et al., 1992]. (b) Results of the geodetic analysis from the discontinuous model. Different patterns of gray indicate the three rigid blocks (inferred boundaries as dashed lines). Arrows: relative movements of blocks (for eastern block, motion relative to central block; for central block, motion relative to western block). Values along lines: calculated length changes from inversion with the discontinuous model (in mm). (c) Histogram: number of lines in network (ordinate) as a function of difference between observed and computed length changes (abscissa, mm/yr).

possible interpretation is that numerous small conjugate strike-slip faults exist, which are mechanically compatible with the regional strain pattern within the Pinanshan Conglomerate. In fact, the results of earlier photo-interpretation as well as the analysis of fault-slip data collected in the field [Barrier *et al*., 1982] showed numerous strike-slip sets affecting in the Pinanshan Conglomerate. This aspect will be discussed in more detail in the next section.

4. Geological evidence of deformation in the Pinanshan Conglomerate

The Pinanshan Conglomerate constitutes an asymmetric synclinal fold (Figure 1b) with a gently inclined western limb and a steeply inclined (sometimes overturned) eastern limb. Along the western limb of the syncline, the Pinanshan Conglomerate is in contact with metamorphic rocks of the Central Range, while on the eastern limb the conglomerate is in contact with the Lichi mélange of the Coastal Range. The strain tensor analysis discussed before indicates a zone of thrusting on the western side of the Pinanshan Conglomerate and a zone of strike-slip faulting on the eastern side. These major faults exposed poorly in the field because of coverage of recent sediments and erosion of river. On the eastern side of Pinanshan Conglomerate, the adjacent Lichi mélange reveals numerous left-lateral fault striations trending NNE-SSW, consistent with strike-slip movement between the Pinanshan Conglomerate and the Coastal Range. However, one outcrop of fault in the eastern edge of the Pinanshan Conglomerate near the Pinantachi shows dip-slip striated slickensides, indicating thrusting of the Coastal Range over the Pinanshan Conglomerate [Barrier *et al*., 1982].

Numerous strike-slip faults, observable at the outcrop scale, have been found in the Pinanshan Conglomerate. The strike-slip faults are commonly associated with conjugate joint sets which are usually marked by streams across steep cliffs and can be easily identified in the field and on the air-photo imagery. Striations on strike-slip fault planes allow to reconstruction of deformation in terms of paleostress [Angelier, 1984]. Barrier *et al*. [1982] first identified strike-slip conjugate joints occurred prior to tilting (folding) of the Pinanshan Conglomerate. After tilting, strike-slip movements continued, including reactivation of the initial conjugate fractures. The paleostress analysis consistently showed that strike-slip faulting occurred under a regime of WNW-ESE (N100°E to N105°E), in a good agreement with the compression that can be expected considering the folding of the Pinanshan syncline (trending approximately N-S to NNE-SSW). The chronology of the strike-slip structures in the Pinanshan Conglomerate implies an extended period of strike-slip stress regime during deformation. Syncline folding and reverse faulting, which undoubtedly occurred under compressional stress regime, associated with prevailed strike-slip faults of outcrop scale suggest a permutation of principal stress axes σ_2/σ_3 occurred within the Pinanshan Conglomerate during compression.

The morphological lineations represent the surface features, which generally reflect recent movements on major structures. We analyzed the morphological lineations and subsequently compared them with the present-day surface deformation revealed by the geodetic data analysis. Two available morphological images have

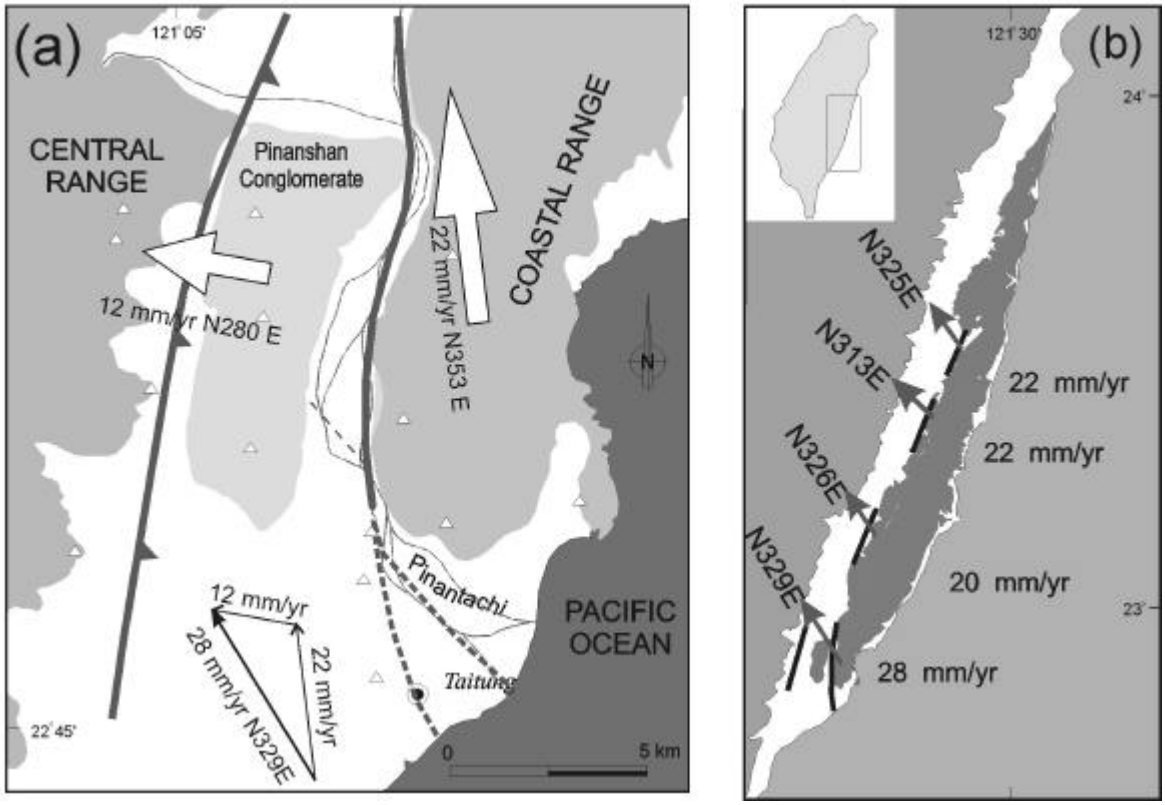

Figure 6. Crustal deformation and displacement deduced from the results of the geodetic data analysis (discontinuous model) and geological observation in the southern Longitudinal Valley, eastern Taiwan. (a) Crustal deformation involves two major faults on both sides of the Pinanshan Conglomerate massif, with additional deformation within the Pinanshan Conglomerate. (b) Application of model of discontinuous deformation along the Longitudinal Valley [Lee and Angelier, 1993]. Arrows indicate displacements of the upthrust, eastern block of the Longitudinal Valley Fault relative to the Central Range. Computed azimuths of displacement in degrees, computed velocity in mm/yr.

been used, the SPOT panchromatic image (Figure 4) which has ground resolution of 10m×10m, and the aerial photographs with a higher resolution of less than 1m×1m. As a consequence, the SPOT image shows regional structural features while the aerial photographs are useful in detailed fracture analysis.

The photo-interpretation of features in the Pinanshan Conglomerate (Figure 7) [Barrier *et al*., 1982] shows two dominant sets of lineations at NW-SE (N140°E) and WNW-ESE (N70°E). The trends of these sets coincide with trends of conjugate strike-slip fault sets observed in the field. This relationship indicates that similar lineations in the Pinanshan Conglomerate likely represent numerous strike-slip faults, which indirectly supports the results of the geodetic data analysis, suggesting substantial deformation within the conglomerate.

South of the Pinanshan Conglomerate, the faults disappear beneath the Taitung plain and offshore. North of the Pinanshan Conglomerate, two branches of the Longitudinal Valley Fault merge into a single major fault towards the Chihshang area (Figure 1) where deformation is concentrated along a narrow zone generally less than 50 m wide [Angelier *et al*., 1997]. The transition of the Longitudinal Valley Fault from a single fault to two fault systems should occur between the Pinanshan Conglomerate and Chihshang.

The evolution of deformation of the Pinanshan Conglomerate can thus be illustrated, based on the structural relationships between the regional folding, thrusting, strike-slip faulting, and the consideration of morphological features: (1) development of conjugate sets of strike-slip joints before tilting (folding) of the Pinanshan Conglomerate; (2) regional asymmetric synclinal folding possibly synchronous with overthrusting by the Lichi mélange of the Coastal Range; (3) conjugate strike-slip faulting following folding including reactivation of the initial conjugate sets of fractures.

5. Discussion

The contact between the Luzon island arc system (the Coastal Range) and the Plio-Pleistocene Pinanshan Conglomerate is presently characterized by a fault zone of left-lateral slip as suggested by the above analyses. However, the existence of the asymmetric Pinanshan Conglomerate syncline with a NNE-SSW fold axis and the steeply inclined eastern limb with nearly vertical layers imply that the unit has been shortened under regional compression trending approximately WNW-ESE (nearly perpendicular to fold axis). Overthrusting by the Coastal Range with NW-SE compression along the eastern boundary of the conglomerate has been documented [Barrier *et al*., 1982]. The

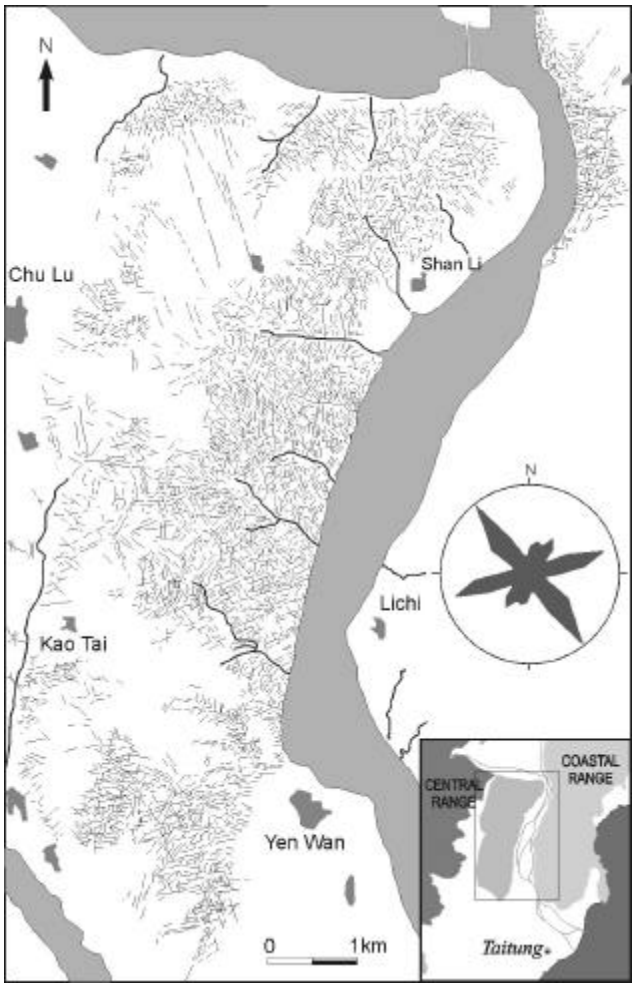

Figure 7. Extraction of alignments from aerial photographs in the Plio-Pleistocene Pinanshan Conglomerate, from Barrier et al. [1982], with rose diagram representing the frequency of trends. Two major preferred orientations (N70°E and N140°E) show conjugate set of fractures, which correspond to the strike-slip faults identified in the field.

orientation of the young fold, the direction of thrusting, and the direction of compression deduced from the paleostress analysis of strike-slip faults all indicate compression stress at a high angle to the active strike-slip suture zone in the southern Longitudinal Valley.

5.1. Kinematics at local and regional scales

The relative motion between the Philippine Sea plate and the Eurasian plate is about 70 mm/yr in the direction of N310°E [Seno *et al.*, 1987]. Recent GPS measurements show a shortening rate of 82 mm/yr across the Taiwan mountain belt between the islands Lanhsu east off Taiwan and the island Penghu in the Taiwan strait west of Taiwan [Yu *et al.*, 1997]. Around southeastern Taiwan, GPS data show shortening of more than 40 mm/yr between the island Lanhsu and the eastern margin of the Central Range [Yu *et al.*, 1997]. Our analysis of discontinuous model from the trilateration networks around the southern Longitudinal Valley reveals a displacement rate of 28 mm/yr in the direction N329°E between the Coastal Range and the Central Range. We conclude that the amount of crustal deformation in the southern Longitudinal Valley accounts for a significant portion of the total convergence between the Philippine Sea plate and the Eurasian plate and is similar to that in the central portion of the valley with shortening rate 21mm/yr in the direction N320°E [Lee, 1994; Angelier *et al.*, 1997].

Paleostress analysis of fault-slip striation in the Pinanshan Conglomerate area [Barrier *et al.*, 1982] revealed a N279°E (N81°W) trending compression, which differs from the direction of total relative displacement between the Coastal Range and the Central Range in the southern Longitudinal Valley (N329°E; Figure 5). However, the N279°E compression is similar to the direction of shortening between the Central Range and the Pinanshan Conglomerate (N280°E), and it is almost perpendicular to the major trend of the suture zone (approximate in N20°E). Thus, it may principally represent the transverse component of the oblique collision along the Longitudinal Valley Fault, because of the partitioning in stress/strain.

5.2. Tectonic evolution of the Pinanshan Conglomerate

The tectonic evolution of the Pinanshan Conglomerate can be summarized as follows. The Pinanshan Conglomerate deposited at the foot of the Central Range when the Luzon island arc system of the Coastal Range approached during the Plio-Pleistocene (Figure 8a). The coarse clastic nature and contents of the Pinanshan Conglomerate resemble that of some youngest layers of the adjacent Takangkou flysch deposits of the Coastal Range [Horng and Shea, 1996], although there is no geological continuity between the two formations,. When the Coastal Range continued to move westward and collided with the Central Range, the Coastal Range was thrusted above the in-between Pinanshan Conglomerate, which began to deform as a faulted syncline (Figure 8b). As these three units (the Coastal Range, the Pinanshan Conglomerate, and the Central Range) were colliding under increasing compression, strain partitioning developed (Figure 8c), the convergence oblique to the boundary being decoupled into strike-slip faulting (on the eastern side of the Pinanshan Conglomerate) and thrusting (on the western side).

6. Conclusions

1. Based on the analysis of geodetic data combined with geological field investigations, we recognize the role of decoupling and partitioning in crustal deformation within an active suture zone of oblique convergence: the southern Longitudinal Valley of eastern Taiwan. Crustal deformation is characterized by the splitting of the Longitudinal Valley fault into two major active branches, resulting in a suture zone composed of three blocks: from east to west, the Coastal Range (the island arc system of Luzon), the Pinanshan Conglomerate (syn-collision molasse deposits), and the Central Range (the metamorphic basement of Eurasia). In contrast, further to the north, the active Longitudinal Valley Fault consists of a single fault with shear concentrating in a very narrow zone [Angelier *et al.*, 1997]. In the southern Longitudinal Valley this fault zone splits into two distinct faults on both sides of the Pinanshan Conglomerate, a thrust fault to the west and a strike-slip fault to the east, exhibiting characteristics of strain partitioning at a convergent plate boundary.

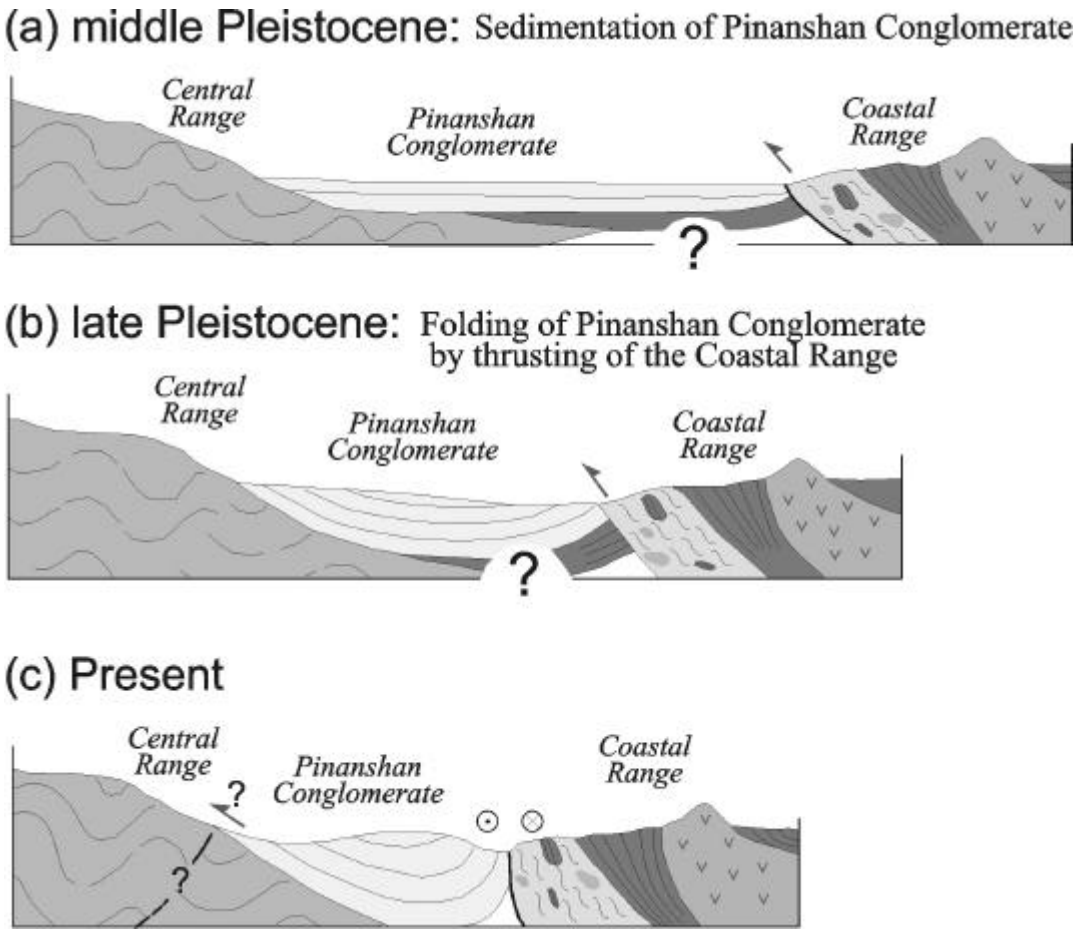

Figure 8. Tectonic evolution of the Pinanshan Conglomerate. (a) Sedimentation of the Pinanshan Conglomerate at the foot of the Central Range during the convergence between the Coastal Range (Luzon island) and the Central Range, during the middle Pleistocene approximately. (b) Late Pleistocene: folding of the Pinanshan conglomeratic layers associated with thrusting of the Coastal Range. (c) Present: the fault across the Longitudinal Valley combines two types of faults: a reverse fault, probably west-vergent, on the western side of the Pinanshan Conglomerate, and a strike-slip fault, left-lateral, on the eastern side.

2. Deformation in the active suture zone of the southern Longitudinal Valley is characterized by a displacement of approximate 28 mm/yr in the direction of about N329°E. The total displacement is decoupled into strike-slip faulting (displacement of 22 mm/yr in the direction N353°E) on the east and thrusting (shortening of 12 mm/yr in the direction N280°E) on the west.

3. Detailed geodetic data analysis indicates that secondary deformation locally occurs within the Plio-Pleistocene Pinanshan Conglomerate. This additional deformation is probably accommodated by numerous sets of conjugate strike-slip faulting (dextral faults trending about N70°E and sinistral ones trending approximately N140°E).

4. The Plio-Pleistocene folding and strike-slip faulting in the Pinanshan Conglomerate indicate a consistent direction of compressional stress, with a compressional stress axis (WNW-ESE) nearly perpendicular to the trends of the major faults (NNE-SSW). This direction of compression is quite consistent with the thrust behavior of the western fault zone. This behavior is made possible by the decoupling along the eastern strike-slip fault, thus illustrates strain/stress partitioning in a transpressive, reverse and left-lateral, stress regime.

Appendix

A1. Strain Tensor Analysis

Within a homogenous deformation domain, we introduce a strain tensor, $\boldsymbol{T}$, representing the crustal deformation. we simply consider the 2-D application, because of the absence of information in the vertical direction (see text). The displacement, $\vec{L}_k$, for a point (x, y) situated at the end of a segment in the network can be obtained by multiplying the strain tensor, $\boldsymbol{T}$, and the vector $\vec{D}_k$ of the coordinate of the point:

$$\vec{L}_k = \boldsymbol{T} \cdot \vec{D}_k \qquad (1)$$

The strain tensor, $\boldsymbol{T}$, is described by three unknowns e_1, e_2 and q, which represent respectively the maximum principal strain, the minimum principal strain in the horizontal plane (positive sign means elongation), and the angle between the e_1 axis and the E-W direction.

$$\boldsymbol{T} = \begin{pmatrix} \cos q & -\sin q \\ \sin q & \cos q \end{pmatrix} \begin{pmatrix} e_1 & 0 \\ 0 & e_2 \end{pmatrix} \begin{pmatrix} \cos q & \sin q \\ -\sin q & \cos q \end{pmatrix} \qquad (2)$$

The calculated displacement, $\vec{L}_k$, is compared with the measured data, $\vec{L}_k^*$. The best-fit strain tensor $\boldsymbol{T}$ is found when the differences between the vectors $\vec{L}_k$ and $\vec{L}_k^*$ are as small as possible. For a network with N lines, we use a least-square approach and search for the average tensor $\boldsymbol{T}$ which provides the smallest sum S:

$$S = \sum_{k=1}^{k=N} (\vec{L}_k - \vec{L}_k^{\,*})^2 \qquad (3)$$

In order to obtain the minimum of S, we set the derivatives $\frac{\partial S}{\partial e_1}$, $\frac{\partial S}{\partial e_2}$ and $\frac{\partial S}{\partial q}$ to zero. Combining with the equations (1), (2) and (3), it results in the following system of equations, where A to F are polynoms depending on the data:

$$\begin{cases} e_1(A + C\cos 2q + B\sin 2q) = D + E\sin 2q + F\cos 2q \\ e_2(A - C\cos 2q - B\sin 2q) = D - E\sin 2q - F\cos 2q \\ (e_1 + e_2)(B\cos 2q - C\sin 2q) = E\sin 2q - F\cos 2q \end{cases} \qquad (4)$$

The solution of these equations gives the values of e_1, e_2 and q. An additional calculation provides the uncertainties $\Delta e_1, \Delta e_2$ and Δq, as functions of the uncertainties of the data of the trilateration network.

A2. Discontinuous Model Analysis

In the discontinuous model [Lee and Angelier, 1993], the deformation is represented by displacements between rigid blocks separated by geological discontinuities (or faults). In this case with two discontinuities, the deformation can be described by ten variables. Deformation for each discontinuity comprises five variables: the vector of relative motion between rigid blocks, including amount (d) and orientation (q), and three variables giving the location of the rectilinear discontinuity.

The vectors of displacement, $\vec{L}_k^*$, for each line in the trilateration network are compared with the calculated vectors, $\vec{L}_k$, produced by the discontinuous model. The sum of the difference, S, between these two vectors, is minimized through a least square approach, for all the segments of the network:

$$S = \sum_{k=1}^{k=N} (\vec{L}_k - \vec{L}_k^*)^2 \qquad (5)$$

In the case of the southern Longitudinal Valley, where two faults are present (i.e., two discontinuities), equation (5) has a more complicated form:

$$S = \sum_{j=1}^{j=M} (\vec{L}_j - \vec{L}_j^*)^2 + \sum_{k=1}^{k=N} (\vec{L}_k - \vec{L}_k^*)^2 + \sum_{t=1}^{t=T} (\vec{L}_t - \vec{L}_t^*)^2 , \qquad (6)$$

where $\vec{L}_j$, $\vec{L}_k$, and $\vec{L}_t$ represent the calculated vectors of displacements along two different discontinuities and the calculated vectors of total displacement (depending on locations of faults relative to stations), while $\vec{L}_j^*$, $\vec{L}_k^*$, and $\vec{L}_t^*$ represent the corresponding vectors from measured data.

In order to fasten the process and to obtain the smallest sum S without considering unrealistic solutions, we limited the possible portions of the discontinuities based on geological observation (see text), and we executed a search process for d_1 (amount of displacement along the first discontinuity) = 1, 2, ….., 40 (in mm/yr), q_1 (orientation of displacement along the first discontinuity) = 1, 2, ..., 360 (in degree), d_2 (amount of displacement along the second discontinuity) = 1, 2, ….., 40 (in mm/yr), q_2 (orientation of displacement along the second discontinuity) = 1, 2, ..., 360 (in degree). We finally obtain the amount (mm/yr) and orientation (azimuth) of displacement along both the discontinuities, as illustrated in Figure 6a.

Acknowledgments. This work was supported by Institute of Earth Sciences, Academia Sinica and National Science Council grant NSC87-2116-M047-002. Helpful suggestions and reviews by J.C. Savage and D.L. Reed greatly improved the manuscript. This is a contribution IESEP98-006 of the Institute of Earth Sciences, Academia Sinica.

References

Angelier, J., Tectonic analysis of fault-slip data sets, *J. Geophys. Res.*, *89*, 5835-5848, 1984.

Angelier, J., H.T. Chu, and J.C. Lee, Shear concentration in a collision zone: kinematics of the active Chihshang Fault, Longitudinal Valley, eastern Taiwan, *Tectonophysics, 247*, 117-144, 1997.

Barrier, E., J. Angelier, H.T. Chu, and L.S. Teng, Tectonic analysis of compressional structure in an active collision zone: the deformation of the Pinanshan Conglomerates, eastern Taiwan, *Proc. Geol. Soc. China, 25*, 123-138, 1982.

Barrier, E., and C. Muller, New observations and discussion on the origin and age of the Lichi Melange, *Memoir of the Geological Society of China, 6*, 303-326, 1984.

Chen, C.H., A preliminary study of the fossil Dinoflagellates from the Tananao Schist, Taiwan (in Chinese), Master thesis, National Taiwan University, 1989.

Chi, W.R., H.M. Huang, and J.C. Wu, Ages of the Milun and Pinanshan Conglomerates and their bearing on the Quaternary movement of eastern Taiwan, *Proc. Geol. Soc. China, 26*, 67-75, 1983.

Fitch, T.J., Plate convergence, transcurrent faulting and internal deformation adjacent to Southeast Asia and Western Pacific, *J. Geophys. Res., 77*, 4432-4460, 1972.

Ho, C.S., A synthesis of the geologic evolution of Taiwan, *Tectonophysics, 125*, 1-16, 1986.

Ho, C.S., *An introduction to the geology of Taiwan (second Edition): explanatory text of the geologic map of Taiwan*, 192 pp., Ministry of Economic Affairs, R.O.C., 1988.

Horng, C.S., and K.S. Shea, Dating of the Plio-Pleistocene rapidly deposited sequence based on integrated magneto-biostratigraphy: a case study of the Madagida-chi section, Coastal Range, eastern Taiwan, *Jour. Geol. Soc. China, 39*, 31-58, 1996.

Horng, C.S., K.S. Shea, and J.C. Lee, Climax of arc-

continent collision in Taiwan: insight from the stratigraphic hiatus of the Coastal Range, in *1997 annual meeting of Geol. Soc. China*, pp. 364-365, Tainan, 1997.

Hsu, T.L., Geology of the Coastal Range, Eastern Taiwan, *Bull. Geol. Surv. Taiwan, 9*, 39-64, 1956.

Hsu, T.L., The Lichi Melange in the Coastal Range framework, *Taiwan, Geol. Surv., Bull, 25*, 87-95, 1976.

Huang, C.Y., P.B. Yuan, S.R. Song, C.W. Lin, C. Wang, M.T. Chen, C.T. Shyu, and B. Karp, Tectonics of short-lived intra-arc basins in the arc-continent collision terrane of the Coastal Range, eastern Taiwan, *Tectonics*, 14, 19-38, 1995.

Jahn, B.M., F. Martineau, J. Peucat, and J. Cornichet, Geochronology of the Taiwan schist complex and crustal evolution of Taiwan, *Mem. Geol. Soc. China, 7*, 383-404, 1986.

Lee, C., and S.B. Yu, Precision of distance measurements for observing horizontal crustal deformation in Taiwan, *Bull. Inst. Earth Sci, Academia Sinica, 5*, 161-174, 1985.

Lee, J.C., and J. Angelier, Location of active deformation and geodetic data analyses: an example of the Longitudinal Valley Fault, Taiwan, *Bull. Soc. Geol. France, 164*, 533-570, 1993.

Lee, J.C., Structure et déformation active d'un orogène: Taiwan, Mem. Sc. Terre, 94-17, 281 pp., Université Pierre et Marie Curie, Paris, 1994.

Mount, V.S., and J. Suppe, State of stress near the San Andreas fault: implications for wrench tectonics, *Geology, 15*, 1143-1146, 1987.

Mount, V.S., and J. Suppe, Present-day stress orientations adjacent to active strike-slip faults: California and Sumatra, *Jour. Geophy. Res., 97*, 11995-12013, 1992.

Page, B.M., and J. Suppe, The Pliocene Lichi melange of Taiwan; its plate-tectonic and olistostromal origin, *Amer. Jour. Sci., 281*, 193-227, 1981.

Seno, T., S. Maruyama, S. Stein, D.F. Wood, C. Demets, D. Argus, and R. Gordon, Redetermination of the Philippine Sea plate relative to the Eurasian plate motion, *Eos, Trans. Am. Geophys. Union, 68*, 1474, 1987.

Stanley, R.S., L.B. Hill, H.C. Chang, and H.N. Hu, A transect through the metamorphic core of the central mountains, southern Taiwan, *Mem. Geol. Soc. China, 4*, 443-473, 1981.

Teng, L.S., and Y. Wang, Island arc system of the Coastal Range, eastern Taiwan, *Proc. Geol. Soc. China, 24*, 99-112, 1981.

Wilcox, R.E., T.P. Harding, and D.R. Seely, Basic wrench tectonics, *AAPG Bull., 57*, 74-96, 1973.

Yang, T.F., J.L. Tien, C.H. Chen, T. Lee, and R.S. Punongbayan, Fission-track dating of the Taiwan-Luzon Arc: eruption ages and evidence for crustal contamination, *J. SE Asia Earth Sci., 11*, 81-93, 1995.

Yen, T.P., C.C. Sheng, and W.P. Keng, The discovery of the Fusuline limestone in the metamorphic complex of Taiwan, *Bull. Geol. Surv., Taiwan*, 23-25, 1951.

Yü, M.S., Present and Recent kinematics of the Pinanshan Conglomerate, eastern Taiwan, in *Annual meeting of Geol. Soc. China, Program and abstracts*, pp. 272-277, Taipei, 1996.

Yu, S.B., and C.C. Liu, Fault creep on the central segment of the longitudinal valley fault, Eastern Taiwan, *Proc. Geol. Soc. China, 32*, 209-231, 1989.

Yu, S.B., D.D. Jackson, G.K. Yu, and C.C. Liu, Dislocation model for crustal deformation in the Longitudinal Valley area, eastern Taiwan, *Tectonophysics, 183*, 97-109, 1990.

Yu, S.B., G.K. Yu, L.C. Kuo, and C. Lee, Crustal deformation in the southern Longitudinal Valley area, eastern Taiwan, *Jour. Geol. Soc. China, 35*, 219-230, 1992.

Yu, S.B., H.Y. Chen, and L.C. Kuo, Velocity field of GPS stations in the Taiwan area, *Tectonophysics, 274*, 41-59, 1997.

Zoback, M.D., et al., New evidences on the state of stress of the San Andreas fault system, *Science, 238*, 1105-1111, 1987.

J. Angelier, Géotectonique (URA 1759), Univ. P. & M. Curie, 4 pl. Jussieu, T26-25-E1, 75252 Paris, France. (ja@lgs.jussieu.fr)

H.-T. Chu, Central Geological Survey, P.O. Box 968, Taipei, Taiwan, R.O.C. (chuht@linx.moeacgs.gov.tw)

J.-C. Hu, J.-C. Lee, and S.-B. Yu, Inst. of Earth Sciences, Academia Sinica, P. O. Box 1-55, Nankang, Taipei, Taiwan 115, (e-mail: jchu@earth.sinica.edu.tw; jclee@earth.sinica.edu.tw; eayusb@ccvax.sinica.edu.tw)

(Received September 18, 1997;
revised June 11, 1998;
accepted July 1, 1998)